



Design of mechanical support of active materials in superconducting generators

Agreement n.:	308974
Duration	November 2012 – October 2017
Co-ordinator:	DTU Wind

The research leading to these results has received funding from the European Community's Seventh Framework Programme FP7-ENERGY-2012-1-2STAGE under grant agreement No. 308974 (INNWIND.EU).



PROPRIETARY RIGHTS STATEMENT

This document contains information, which is proprietary to the "INNWIND.EU" Consortium. Neither this document nor the information contained herein shall be used, duplicated or communicated by any means to any third party, in whole or in parts, except with prior written consent of the "INNWIND.EU" consortium.

Document information

Document Name:	Design of mechanical support of active materials in superconducting generator
Document Number:	Deliverable D3.43
Author:	Asger B. Abrahamsen
Document Type	Report
Dissemination level	PU
Review:	Henk Polinder
Date:	1 November 2017
WP:	Electromagnetic conversion
Task:	Task 3.1
Approval:	Approved by WP Leader

TABLE OF CONTENTS

TABLE OF CONTENTS	3
1 INTRODUCTION.....	4
1.1 Superconducting generators design philosophies.....	4
1.2 Light weight and not too expensive	4
1.3 Cheap and not too heavy.....	4
1.4 State of the art	5
2 MECHANICAL SUPPORT OF MGB ₂ COIL OF TASK 3.13.....	7
2.1 Electromagnetic design of 10 MW MgB ₂ generator.....	7
2.2 Mechanical support of MgB ₂ coil	7
2.2.1 INNWIND.EU MgB ₂ race track demonstration coil	12
2.3 Air cored coil with steel support plate.....	13
2.4 Discussion	19
2.5 Conclusion on air cored coil support.....	19
3 MECHANICAL SUPPORT OF MGB ₂ COILS IN 10 MW GENERATOR	20
3.1 Scaling of the SUPRApower cryostat to the INNWIND.EU generator.....	21
4 DISCUSSION	24
5 CONCLUSION	25
REFERENCES	26

1 INTRODUCTION

1.1 Superconducting generators design philosophies

This report holds the findings of the deliverable D3.43 “Design of mechanical support of the active materials in superconducting generators” which is part of the work package on electromagnetic conversion (WP3) of the INNWIND.EU project.

In order to use the superconductors in wind turbine generators one will have to keep the superconducting coils in place inside a cryostat, which is the enclosure of the coil providing the thermal insulation to maintain an operation temperature in the order of 10-30 K (- 263 to - 243 °C). This cold temperature is needed, because the superconductors will have a vanishing electrical resistance as long as they are cooled below what is called the critical temperature T_c , where the free electrons of superconductors are bound into pairs of two electrons. Secondly the magnetic field B produced by the coils of a superconducting generator tend to create quantized microscopic vortex flows of the electron pairs, whereby the critical current density J_c of the superconductor is suppressed.

The superconducting coils of a wind turbine generator will also experience large Lorentz forces on the superconducting wires and the present report is examining how to support these Lorentz forces and how to support the coils without introducing too much heat into the coils.

The Task 3.1 on superconducting generators in the INNWIND.EU project started out with investigation of a design philosophy of providing “a light weight generator that should not be too expensive”, but it has turned out that the economical advantage of providing a light weight generator for the INNWIND.EU 10 MW reference turbine and foundation for 50 m of water is not as high as expected. The main argument is that the resonance frequencies of the entire structure comprising the turbine and the foundation is calling for a higher top head mass in order to move the resonance away from the 3p excitation of the turbine. Thus the design philosophy of the superconducting generators has been changed for the work of task 3.1 to examine a “cheap but not too heavy” superconducting generator (Abrahamsen, Liu, & Polinder, Direct drive superconducting generators for INNWIND.EU wind turbines, 2017). The implication of this change of the design philosophy on the mechanical support and the cryostat of the superconducting coils will be outlined below.

1.2 Light weight and not too expensive

The main driver for designing superconducting generators is the possibility to provide a lot of amp-turns in compact windings, whereby the amount of silicon steel needed to close the magnetic flux path in a wind turbine generator pole can be reduced. This holds the potential for a significant weight reduction, because the superconductors can give magnetic flux densities exceeding the saturation magnetization of the silicon steel. However that comes with the need of using more superconductors and thereby also a more expensive generator.

A consequence of this design is that the superconducting coil will most likely not hold a magnetic core of silicon steel in order to reduce the cold mass that needs to be cooled down. The superconducting coils can be placed in one large tube shaped cryostat, which needs to be equipped with a torque tube transferring the torque from the cold coils and to the warm shaft.

1.3 Cheap and not too heavy

By using cost as the primary design driver of the generator design, the superconducting generator tends to use as little superconductor as possible by replacing expensive superconductor by cheap iron. This is driving up the weight, but as long as the weight is not getting too high compared to the rest of the nacelle component, it will probably be possible to integrate the design in the nacelle.

The consequence of this design philosophy is that a warm silicon iron core is desirable to go through the centre of the superconducting coils. Thus the cryostat for the superconducting coils must have a large hole in the middle and will be placed around a rotor silicon iron structure. Such cryostats might be more difficult to manufacture, but an advantage might be a modular design allowing the replacement of one superconducting coil if it is damaged.

A major concern is however that such superconducting machines are very similar to conventional machines based on permanent magnets (PM), whereby they will have a hard time to become economical competitive with the PM direct drive generator technology. This has been indicated by a scenario study of the MgB₂ generator of deliverable D3.11 (Abrahamsen, Liu, & Polinder, Direct drive superconducting generators for INNWIND.EU wind turbines, 2017), where the Levelized Cost of Energy (LCoE) and the weight of the 10 MW MgB₂ generator were investigated for the current cost and properties of the MgB₂ wire from Columbus Superconductors as shown in Figure 2-1. It was found that an iron cored generator topology was the cheapest, but at the same time that it was also heavier than the permanent magnet direct drive generator. The question also posed was what if the cost of the MgB₂ is reduced to 1/4, if the critical current density $J_c(B)$ of the wire is improved by a factor of 4 and finally what if both the cost is reduced and the properties are increased in the future (Liu, Polinder, Abrahamsen, & Ferreira, 2017). It was found that the Levelized Cost of Energy (LCoE) of the different topologies ranging from air cored and to iron cored machines would be very similar for the improved MgB₂ scenarios and topologies with better mass scaling will therefore become possible. Thus it is expected that the topology of the superconducting generators will change in the future as the superconductors will improve and this will most likely also mean that the down selection of a winner topology is currently hard to make. This also has the consequence that the down selection of the winner cryostat design is also hard to make. This report will therefore reflect the cryostat design for an air-cored generator even though that the INNWIND.EU MgB₂ 10 MW and 20 MW generators in Deliverable D3.11 (Abrahamsen, Liu, & Polinder, Direct drive superconducting generators for INNWIND.EU wind turbines, 2017) are based on the iron cored topology.

1.4 State of the art

The state of the art of MgB₂ superconductor based wind turbine generators has recently been reviewed by Abrahamsen (Abrahamsen, Wind generator projects based on MgB₂ superconductors, 2016). It was found that several design approaches have been investigated by different researchers and organizations. There are 3 major types of machines proposed:

- 1) Partial superconducting direct drive wind turbine generators with the field coils made of MgB₂ wire and the armature being a conventional copper winding wound around silicon steel.
- 2) Transverse flux wind turbine generators using an MgB₂ circular winding to magnetize the generator structure based on magnetic steel and copper windings.
- 3) Fully superconducting wind turbine generators, where both the field and armature windings are based on MgB₂ wire.

Option 1) has been used for the initial design of the 10 MW MgB₂ generator of the INNWIND.EU project (Abrahamsen, et al., 2014). That design was then used to design a scaled version of an MgB₂ coil with the purpose to demonstrate the MgB₂ coil technology (Abrahamsen, Magnusson, Jensen, Liu, & Polinder, 2014). The EU FP7 project SUPRApower has also investigated this option for at 10 MW wind turbine design and conducted a large amount of work on the demonstration of the cryostat and cooling system (Marino, Pujana, & Sarmiento, 2016) and (Sun, Sanz, & Neumann, 2015).

Option 2) has been proposed by Keysan *et. al.* and is providing a generator of relatively low mass, but is based on using magnetic steel with a 50 % share of cobalt (Keysan & Mueller, 2015). This

will probably drive up the cost of the generator compared the current permanent magnet direct drive technology.

Option 3) has been proposed by S. Kalsi in collaboration with the American MgB₂ wire manufacturer Hypertech (Kalsi, 2014). The concept holds the potential to provide a compact generator at a relatively low cost. The wire for making a superconducting armature winding does however not yet seem to be available on the market. Finally a fully superconducting wind turbine generator based on the double helix coil winding technique has been proposed by American Magnetic Lab (AML, 2017). Again it seems that the wire for constructing the armature is not readily available.

This report primarily holds the investigation of the structural aspect of the support of the MgB₂ coil for the demonstration of task 3.13 “Fabrication of MgB₂ coils” (Magnusson, Hellesø, Paulsen, Eliassen, & Abrahamsen, 2016). It will however also hold a preliminary design of the final cryostat for an MgB₂ generator following the design philosophy: “Cheap and not too heavy”. This configuration is however close to the concept proposed by Technalia for the SUPRApower project and their already published work will be transferred to the INN WIND.EU MgB₂ generators in order not to duplicate the work of SUPRApower. The latter is used in deliverable D3.11 to make the economical assessment of the INN WIND.EU MgB₂ generators and turbines (Abrahamsen, Liu, & Polinder, Direct drive superconducting generators for INN WIND.EU wind turbines, 2017).

2 MECHANICAL SUPPORT OF MgB_2 COIL OF TASK 3.13

2.1 Electromagnetic design of 10 MW MgB_2 generator

The design of the 10 MW MgB_2 generator was first done with the intention to provide a lightweight design and the total amount of superconducting MgB_2 wire used ended up being 475 km (Abrahamsen, Magnusson, Jensen, Liu, & Polinder, 2014) (Magnusson, Hellesø, Paulsen, Eliassen, & Abrahamsen, 2016). This design is based in on air-cored superconducting field windings and an armature winding without magnetic teeth. It was known that such a design would provide the upper limit of how much superconductor that must be used in a 10 MW wind generator and any improvement in design would most likely decrease the amount of superconductor used and thereby also the cost of the machine.

This design was used to specify the MgB_2 demonstration coil of task 3.13 (Magnusson, Hellesø, Paulsen, Eliassen, & Abrahamsen, 2016) by simply down scaling the length of the coil from 3.1 m to 0.5 m, but keeping the cross sectional dimensional the same. In this way the coil demonstration is testing if all aspects of winding large MgB_2 coils suited for a wind turbine generator of 10 MW power rating.

The MgB_2 demonstration coil is a race track coil with circular end windings between straight sections. It is made by stacking 10 double pancake coils on top of one another and serial connecting the 10 pancake coils into one winding.

From a mechanical point of view there are several challenges that must be taken into account for the demonstration of the MgB_2 coil:

- 1) The Lorentz forces on the wires of the coil must be supported on the straight section of the coil by placing stainless steel plates on the sides.
- 2) The temperature distribution of the coil must be sufficiently homogenous in order not to get a local decrease of the critical current density.
- 3) The thermal contraction of different materials should not cause stresses that can damage the wire, whereby critical current properties might be decreased.

2.2 Mechanical support of MgB_2 coil

The primary concern for the coil support is to ensure that the MgB_2 wire is not exposed to an axial stress larger than $\sigma_{critical} = 110$ MPa and a strain of $\epsilon_{critical} = 0.15$ %, because this will break the connection between the MgB_2 metal alloy grains in the composite wire shown in Figure 2-1. Secondly the wire must not be bended to a diameter smaller than the critical bending diameter, which is $D_{bend,critical} = 150$ mm. These parameters obtained from Columbus Superconductors (Columbus Superconductors, 2017) are listed in Table 2-1.

The MgB_2 demonstration coil was designed with an inner opening of the race track coil being two times the critical bending diameter of the wire, whereby the criteria of the bending diameter should be no problem to fulfil (see Figure 2-2). The additional constrains on the stress and strain will however need further analysis. This will be done by first introducing a very simple analytical model and then to perform a detailed Finite Element analysis.

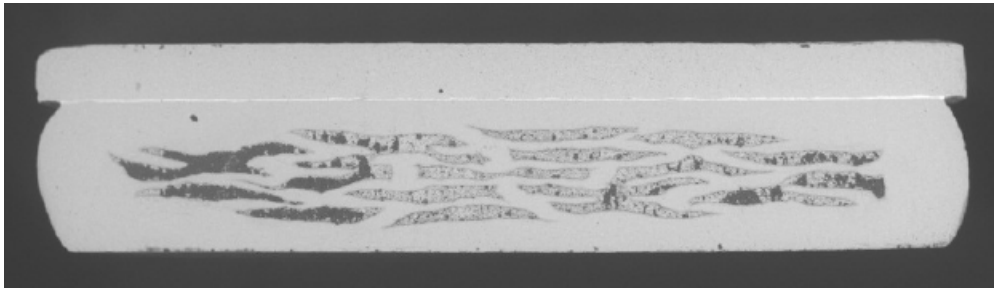


Figure 2-1 Scanning Electron Microscope (SEM) image of the cross section of the multifilament MgB₂ wire used for the MgB₂ coils demonstration of INN WIND.EU. Black areas are the MgB₂ filament embedded in a nickel matrix and the top strip is made of Cu to provide thermal stability. The width and thickness of the wire is 3.0 mm x 0.7 mm. Reproduced from the deliverable report D3.13 of the INN WIND.EU project (Magnusson, Hellesø, Paulsen, Eliassen, & Abrahamsen, 2016).

Materials	Dimension	%
MgB ₂ [mm ²]	0.34	21.5
Nickle [mm ²]	1.24	78.5
Total SC-wire [mm ²]	1.58	100
SC-wire cross section [mm]	3.0 x 0.5	
Copper strip section [mm]	3.0 x 0.2	
Total wire cross section [mm]	3.0 x 0.7	
Critical bending diameter [mm]	150	
Critical tensile stress [MPa]	110	
Critical tensile strain [%]	0.15	

Table 2-1 MgB₂ wire dimensions and mechanical critical parameters

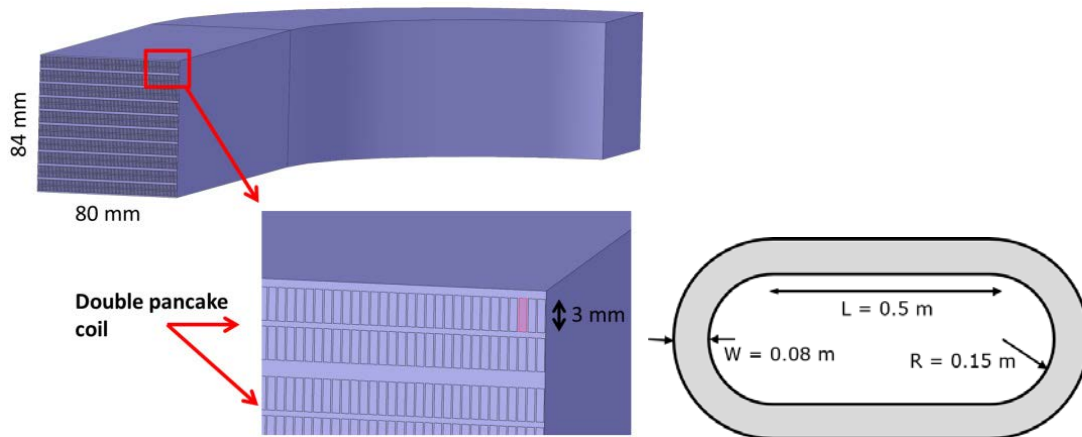


Figure 2-2 Left: Illustration of the internal structure of the MgB₂ demonstration race track coil of the INN WIND.EU project. The top shows a cut of the race track coil composed of 10 double pan cake coils stacked on top of one another. The radius of the end section is 15 cm and the cross sectional dimensions of the race track coil are 84 mm tall and 80 mm deep. The lower image is showing a zoom of the top corner, where the individual MgB₂ wires can be seen. Right: Illustration of the overall dimension of the race track coil.

The first concern in evaluating the stress and strain of the MgB₂ racetrack coil is to supply some mechanical support to the outside of the straight sections of the race track, because the Lorentz forces acting on the wires will tend to push the coil shape into a circle. Figure 2-3 is showing a simple model of how to support the two sides of the race track coil, which is represented as two

infinitely long square shaped conductors. These conductors are supported by steel plates, which are held together by rods or plates resulting in a spring force that is counter balancing the Lorentz force between the two conductors.

The magnetic flux density \mathbf{B} created by the current density \mathbf{J} in conductors can be found from Maxwell's equations quite easily if the conductors are considered as round

$$\nabla \times \mathbf{B} = \mu_0 \mathbf{J} \Rightarrow B_{\theta,1} = \frac{\mu_0 I_1}{2\pi r_1} \quad (1)$$

where μ_0 is the vacuum permeability, $B_{\theta,1}$ is the azimuthal magnetic flux component in a distance r_1 from the round wire holding a total current of I_1 . Since Maxwell's equations are linear if there are no materials with a magnetization, the total magnetic flux density can be found by adding two terms like eq. (1) for both straight sections of the race track. This is the case of the race track demonstration coil, but will not be true if the coil is mounted in a generator with magnetic steel, where finite element methods should be used.

The center magnet flux density of the coil when neglecting the end windings will be

$$B_{center} = \frac{\mu_0 I_1}{2\pi r_1} + \frac{\mu_0 I_2}{2\pi r_2} = \frac{\mu_0 I_{coil}}{\pi x_0} \quad (2)$$

where x_0 is the position of the coil conductor center as shown on Figure 2-3 and the coil current is denoted $I_{coil} = I_1 = I_2$.

In order to evaluate if the superconductor is exposed to a magnetic flux density which is exceeding the critical field of the wires, it is instructive to calculate the magnetic field strength on the inner edge of one of the wires

$$B_{edge} \left(x_0 - \frac{w}{2} \right) = \frac{\mu_0 I_1}{2\pi \frac{w}{2}} + \frac{\mu_0 I_2}{2\pi \left(2x_0 - \frac{w}{2} \right)} = \frac{\mu_0 I_{coil}}{\pi w} \left(\frac{1}{1 - \frac{w}{x_0}} \right) \quad (3)$$

where w is the width of the coil cross section and x_0 is the position of the coil conductor center as shown on Figure 2-3 and the coil current is denoted $I_{coil} = I_1 = I_2$.

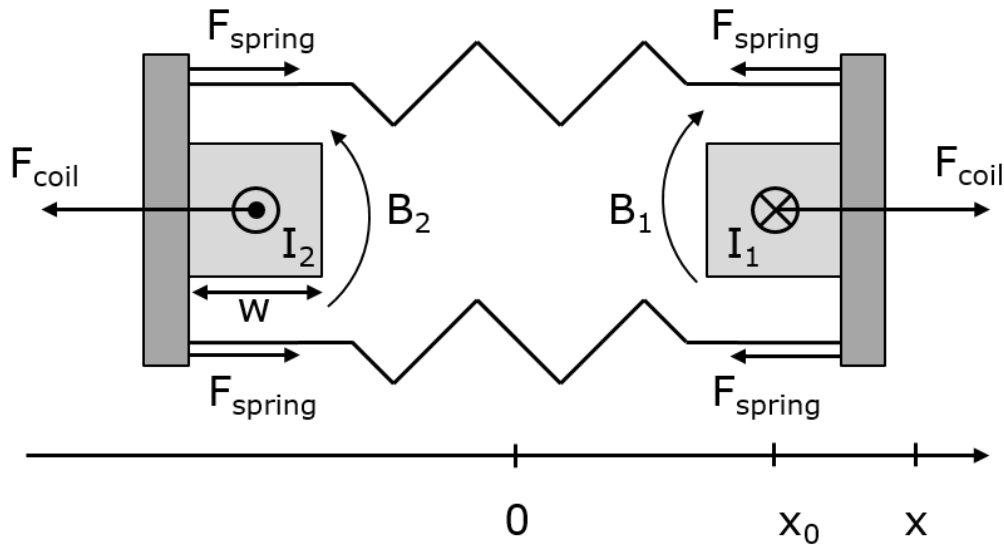


Figure 2-3 Illustration of force F_{coil} action on the two straight sections of an infinitely long race track coil, where the two conductors are holding the current I_1 and I_2 of equal size but opposite direction. The coil sections are supported by two plates, which are hold together by support rods providing the spring force F_{spring} .

The Lorentz force on the wire with index 2 due to the magnetic flux density created by the wire with index 1 is given by

$$\mathbf{F}_{21} = I_2 \int d\mathbf{l} \times \mathbf{B}_1 \quad (4)$$

where the integration is done over the conductor line element $d\mathbf{l}$ holding a current I_2 and where the magnetic field \mathbf{B}_1 from wire 1 is present.

By combing eq. (1) and eq. (4) one can obtain the following expression for the coil force F_{coil}

$$F_{coil} = I_2 l \frac{\mu_0 I_1}{2\pi r_1} = \frac{\mu_0 l_{coil} I_{coil}^2}{2\pi 2(x-\frac{w}{2})} \quad (5)$$

where the coil current $I_{coil} = I_1 = I_2 = I_{wire} \times N_{wire}$ with I_{wire} being the current in each wire of the coil and N_{wire} is the number of turns in the coil. l_{coil} is representing the length of the straight section of the race track coil.

In order to determine the new equilibrium position of the coil sections in Figure 2-3 one has to balance the Lorentz forces on the coil with the spring force on the coil support, which is given by

$$F_{spring} = -k(x - x_0) \quad (6)$$

where x_0 is the unloaded outer position of the straight section and k is the spring constant.

Newton's second law then gives

$$ma = F_{coil} + F_{spring} = 0 \Rightarrow \quad (7)$$

$$\frac{\mu_0 l_{coil}^2}{2\pi} \frac{1}{2(x-\frac{w}{2})} = k(x - x_0) \Rightarrow \quad (8)$$

$$x = \frac{x_0 + \frac{w}{2} \pm \sqrt{\left(x_0 + \frac{w}{2}\right)^2 - 4\left(x_0 \frac{w}{2} - \frac{\mu_0 l_{coil}^2}{2\pi} \frac{1}{2k}\right)}}{2} \quad (9)$$

The relative change ε of the equilibrium position of the coil straight section can be written as

$$\varepsilon = \frac{x - x_0}{x_0} = \frac{\frac{w}{2} - x_0 \pm \sqrt{\left(x_0 + \frac{w}{2}\right)^2 - 4\left(x_0 \frac{w}{2} - \frac{\mu_0 l_{coil}^2}{2\pi} \frac{1}{2k}\right)}}{2x_0} \quad (10)$$

The spring constant k can be related to the cross sectional area A of the support rods with a length L_0 used to keep the two straight sections together.

$$F = \sigma A = E\varepsilon A = \frac{EA}{L_0} \Delta x = k\Delta x \Rightarrow k = \frac{EA}{L_0} \quad (11)$$

where E is the elastic modulus of the support rods with a length of L_0 .

The end sections of the coil are changed from circles and into ellipses if the straight sections are moved apart as illustrated in Figure 2-4. In order to estimate if the tensile strain of the wires are exceeding the critical strains one has to relate the movement of the straight sections to an expansion of the perimeter length of the elliptical end section. The perimeter of an ellipse can be approximated as

$$p \approx \pi(a + b) \quad (12)$$

where a and b are the minor and major axis of the ellipse. The major axis b is related to the movement of the straight sections by

$$b = a(1 + \varepsilon) \quad (13)$$

where ε is given by eq. (10) and

$$p_\varepsilon \approx 2\pi a \left(1 + \frac{\varepsilon}{2}\right) \quad (14)$$

The relative strain of the wire in the elliptical section then becomes

$$\varepsilon_p = \frac{p_\varepsilon - p_0}{p_0} = \frac{2\pi a \left(1 + \frac{\varepsilon}{2}\right) - 2\pi a}{2\pi a} = \frac{\varepsilon}{2} \quad (15)$$

This can be used to specify a critical strain of the wire and then to relate that to a strain of the straight section. By inverting equation (10) one can obtain an equation for the spring constant and thereby the dimension of the support rods that will be needed to prevent the superconducting coil from opening up too much and thereby strain the superconducting wires at the end section.

The equation for the spring constant is

$$k = \frac{\mu_0}{2\pi} \frac{l_{coil}^2}{x_0 \frac{w}{2} \frac{1}{4} \left[\left(x_0 + \frac{w}{2}\right)^2 - \left(4x_0 \varepsilon_p + x_0 - \frac{w}{2}\right)^2 \right]} \quad (16)$$

which can now be used to find the cross sectional area A_{cross} of the supporting steel bars using eq. (10)

$$A_{cross} = \frac{L_0 k}{E} \quad (17)$$

where E is the elastic modulus of the support material of length L_0 .

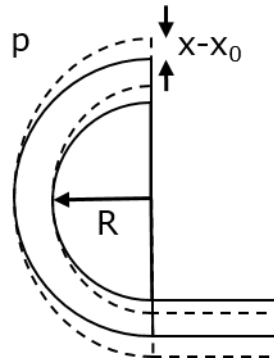


Figure 2-4 Illustration of deformation of end sections of the race track coil as the straight sections are moved outwards to x from x_0 . The perimeter of the elliptical end-section is denoted p and the minor axis of the ellipse is given by the radius R of the initial circular end section.

2.2.1 INN WIND.EU MgB₂ race track demonstration coil

The INN WIND.EU MgB₂ race track coil have the following parameters:

$I_{wire} =$	130 - 150 A
$N_{wire \text{ per DP}} =$	$2 \times 80 \text{ mm} / (0.7 \text{ mm} + 0.05 \text{ mm}) = 212$
$N_{wire \text{ race track}} =$	$10 \times N_{wire \text{ per DP}} = 2120$
$I_{coil} =$	$N_{wire} \cdot I_{wire} = 277 - 320 \text{ kA-turns}$
$w =$	80 mm
$H_{winding} =$	84 mm
$R_{end} =$	150 mm
$x_0 =$	$R_{end} + w/2 = 150 \text{ mm} + 40 \text{ mm} = 190 \text{ mm}$
$L_{straight} =$	500 mm
$\epsilon_p =$	0.075 % (as specified by the wire manufacturer)

This result in a magnetic field at the centre and at the edge of the coil

$B_{center} =$	0.58 - 0.67 T
$B_{edge} =$	2.4 - 2.8 T

Giving repulsive forces in the order of

$F_{coil} =$	25.6 - 34.1 kN (2 - 3 tons on the 0.5 m of straight section)
--------------	---

This will need a stainless steel support of the straight section with a thickness of

$t_{stainless} =$	7 - 9 mm
-------------------	----------

if the elastic modulus of the steel is assumed to be $E = 200 \text{ GPa}$.

Thus it is estimated that about 4-5 mm of stainless steel is needed on both sides of the coil to keep the deformation below the critical strain.

The resulting pressure acting on the coil is

$$P_{\text{coil}} = F_{\text{coil}} / (L_{\text{straight}} \times H_{\text{winding}}) \sim 0.6 - 0.9 \text{ MPa}$$

which is considerable lower than the critical tensile stress of the MgB_2 wire given as 110 MPa.

It should be noted that the centre magnetic field is about half of what was specified for the 10 MW MgB_2 race track coil in (Abrahamsen, Magnusson, Jensen, Liu, & Polinder, 2014). This is due to a lower operation current, because the cooling of the MgB_2 race track coil ended up at $T \sim 20 \text{ K}$ compared to the design temperature of $T = 10 - 15 \text{ K}$ specified in the paper. Secondly the center field in the paper is based on having back iron behind the copper armature windings in the 10 MW generator.

2.3 Air cored coil with steel support plate

A proposal on an air cored race track supported by a steel cover was designed for the MgB_2 race track coil in order to provide a separate unit that could be tested and then later integrated into a rotor structure. Figure 2-5 is showing the coil and the support structure connected to the cold head RDK408 sitting in the test cryostat of SINTEF. At the top one can see the room temperature part of the cold head mounted into the cryostat wall (square plate). The plate below is part of the radiation shield of the cryostat and is cooled down to about $T = 80 \text{ K}$ by the first cooling stage of the cold head. The coil is hanging in glass fibre plates (yellow), which are placed on both side of the coil. The glass fibre plates are attached to the coil by two glass fibre rods going through the steel support plates and through two inner glass fibre supports of the top end section of the coil. The coil is thermally supported by two copper plates extending up to the second stage of the cold head which is at $T \sim 12-15 \text{ K}$. Thus all heating generated in the coil is conducted from the coil and up into the cold head, which will have to remove that heat. Secondly all heat radiated or conducted into the coil will also have to be removed this way.

The mechanical support of the coil is made by placing two stainless steel 316 plates on the straight section edge of the coil and placing a stainless steel cover of about 5 mm thickness over the two sides of the coil (similar to the illustration of Figure 2-3).

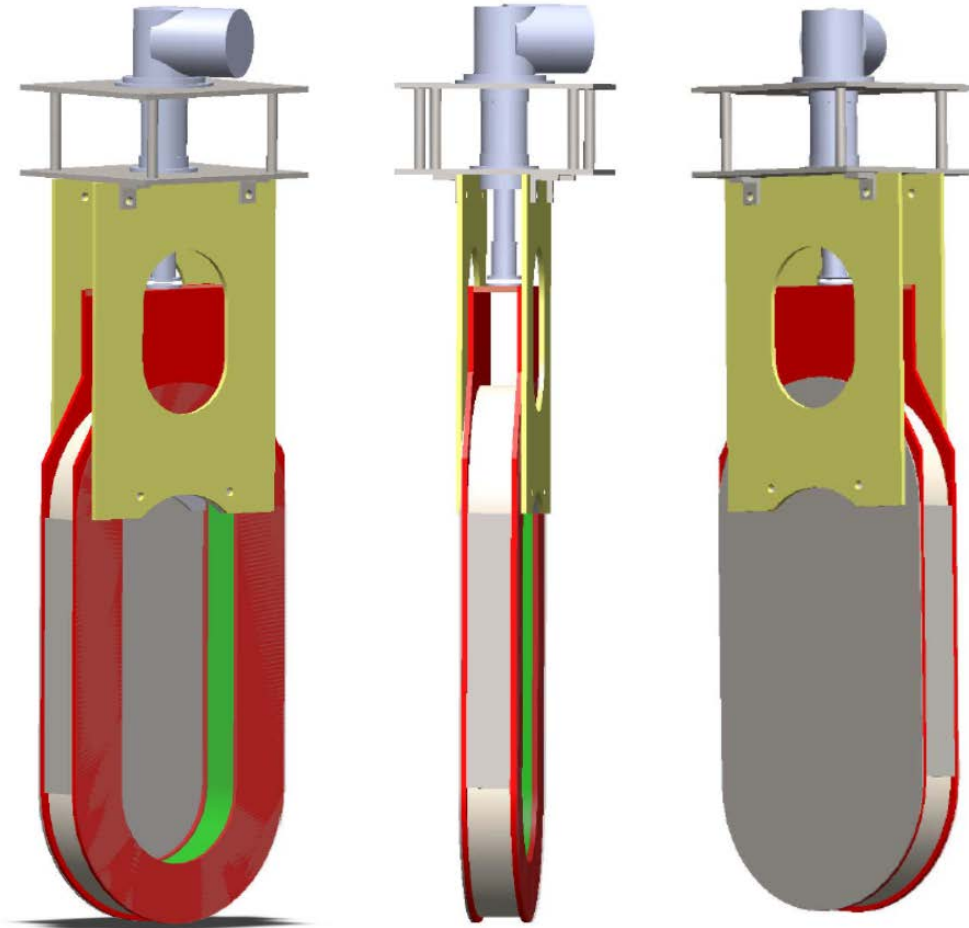


Figure 2-5 Mechanical and thermal support of the MgB₂ race track demonstration coil.

A major concern about this configuration is the thermal contraction of the different materials as they are cooled down. In order to clarify that the Solidworks drawing of the coil and the support were exported to the finite element simulation tool COMSOL in order to determine the coupling between the temperature distribution, the thermal contraction and the Von Mises stresses.

The properties of the materials were describes as copper, stainless steel and nickel to represent the thermal support, mechanical support and the MgB₂ coil winding respectively. The properties are listed in Figure 2-6, Figure 2-7 and Figure 2-8. Figure 2-9 and Figure 2-10 shows the linear thermal coefficient of expansion and the thermal conductivity as function of temperature and how appropriate numbers are selected for T = 30 K. The latter temperature is selected because the thermal contraction below 30 K is very small, whereby T = 30 K is a good representation of the thermal contraction from room temperature and to temperatures below T = 30 K (The MgB₂ operation temperature is lower than T = 30 K, but all contractions have taken place once the temperature reaches 30K).

Figure 2-11 is showing the temperature distribution of the coil cooled to T = 30 K and with a heat dissipation of 1 W distributed evenly over the coil volume. A temperature different of about ½ K is seen and is seen to prove that the 10 mm of Cu thermal support plate is enough to provide god thermal stability of the coil.

Figure 2-12 is showing a displacement of about 2 mm of the coil lower end section as it is cooled down. In the MgB₂ coil demonstration the hanging coil support will allow the coil to move and it is therefore not considered an issue.

Figure 2-13 is now showing the Von Mises stress due to the thermal stress. It is seen that the maximum of the scale bar is reaching 372 MPa, which is considerable more than the critical tensile stress of the wire. It should however be noted that this stress level is observed in the connection line where the coil domain is intersecting with the support bar as shown in Figure 2-14. Thus the high maximum value is an artefact of a difficult meshing region. The general stress level is about 30-60 MPa, whereby the MgB₂ wire is not pushed to the critical limit.

Property	Name	Value	Unit	Property group
✓ Coefficient of thermal expansion	alpha	11.94e-6[1/K]	1/K	Basic
✓ Heat capacity at constant pressure	Cp	385[J/(kg*K)]	J/(kg·K)	Basic
✓ Density	rho	8700[kg/m^3]	kg/m ³	Basic
✓ Thermal conductivity	k	950[W/(m*K)]	W/(m·K)	Basic
✓ Young's modulus	E	110e9[Pa]	Pa	Young's modulus and Poisson's ratio
✓ Poisson's ratio	nu	0.35	1	Young's modulus and Poisson's ratio
Relative permeability	mur	1	1	Basic
Electrical conductivity	sigma	5.998e7[S/m]	S/m	Basic
Relative permittivity	epsilon _{nr}	1	1	Basic
Reference resistivity	rho ₀	1.72e-8[ohm*m]	Ω·m	Linearized resistivity
Resistivity temperature coefficient	alpha	0.0039[1/K]	1/K	Linearized resistivity
Reference temperature	Tref	298[K]	K	Linearized resistivity

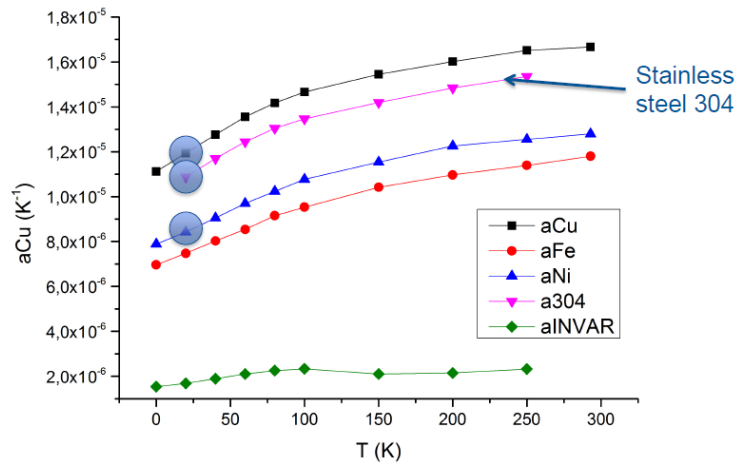
Figure 2-6 Properties of copper in the thermal stress simulation

Property	Name	Value	Unit	Property group
✓ Coefficient of thermal expansion	alpha	10.88e-6[1/K]	1/K	Basic
✓ Heat capacity at constant pressure	Cp	475[J/(kg*K)]	J/(kg·K)	Basic
✓ Density	rho	7850[kg/m^3]	kg/m ³	Basic
✓ Thermal conductivity	k	3[W/(m*K)]	W/(m·K)	Basic
✓ Young's modulus	E	205e9[Pa]	Pa	Young's modulus and Poisson's ratio
✓ Poisson's ratio	nu	0.28	1	Young's modulus and Poisson's ratio
Relative permeability	mur	1	1	Basic
Electrical conductivity	sigma	4.032e6[S/m]	S/m	Basic
Relative permittivity	epsilon _{nr}	1	1	Basic

Figure 2-7 Properties of stainless steel in thermal stress simulation

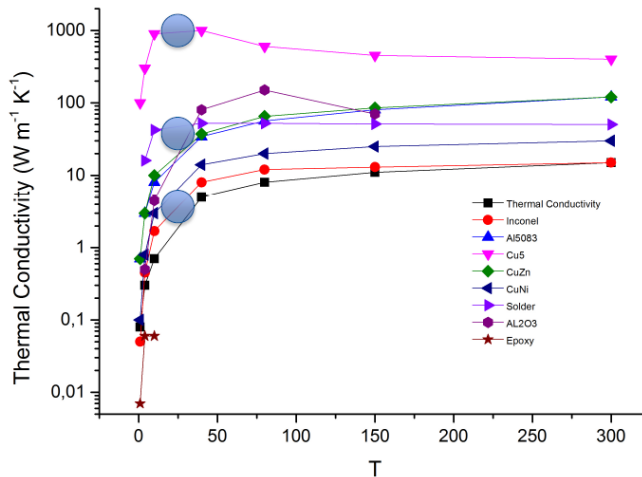
Property	Name	Value	Unit	Property group
✓ Coefficient of thermal expansion	alpha	8.42e-6[1/K]	1/K	Basic
✓ Heat capacity at constant pressure	Cp	440[J/(kg*K)]	J/(kg·K)	Basic
✓ Density	rho	7870[kg/m^3]	kg/m ³	Basic
✓ Thermal conductivity	k	30[W/(m*K)]	W/(m·K)	Basic
✓ Young's modulus	E	33e9[Pa]	Pa	Young's modulus and Poisson's ratio
✓ Poisson's ratio	nu	0.33	1	Young's modulus and Poisson's ratio
Relative permeability	mur	4000	1	Basic
Electrical conductivity	sigma	1.12e7[S/m]	S/m	Basic
Relative permittivity	epsilon _{nr}	1	1	Basic

Figure 2-8 Properties of nickel in thermal stress simulation



G. K. White, "Exp tech in low temp physics" (1979), table F
 Abrahamsen, DTU Wind Energy, 23 April 2015

Figure 2-9 Linear coefficient of expansion of different metals as function of temperature. Appropriate numbers for Cu, stainless steel and Ni at T = 30 K were used in the simulation.



G. K. White, "Exp tech in low temp physics" (2002), table B.6
 Abrahamsen, DTU Wind Energy, 23 April 2015

Figure 2-10 Thermal conductivity of construction materials used for cryogenic supports as function of temperature. Appropriate numbers for Cu, stainless steel and Ni at T = 30 K were used for the thermal stress simulation.

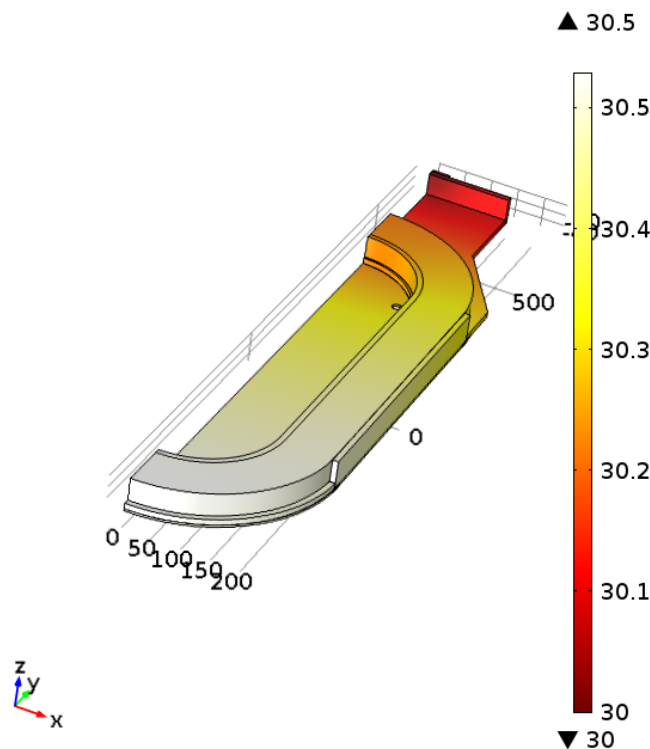


Figure 2-11 Temperature distribution of the coil and thermal support when a heat dissipation of 1 W is distributed evenly in the coil and conducted to the cold head mounted on top of the plate at the top. Only $\frac{1}{4}$ of the geometry is calculated to improve computational efficiency. The scale is temperature [K].

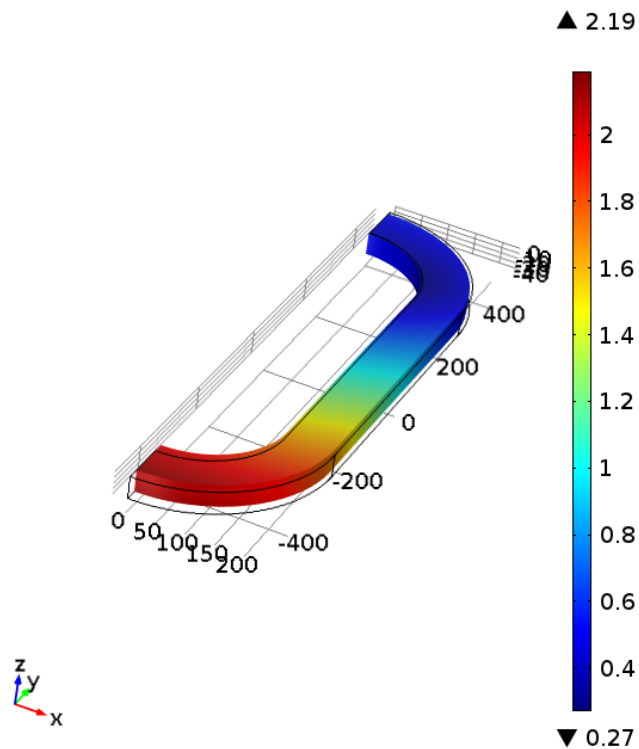


Figure 2-12 Displacement of the coil after cooling it down from room temperature to $T = 30$ K. The displacement is shown in the unit of [mm]. Only the coil domain is shown in the figure.

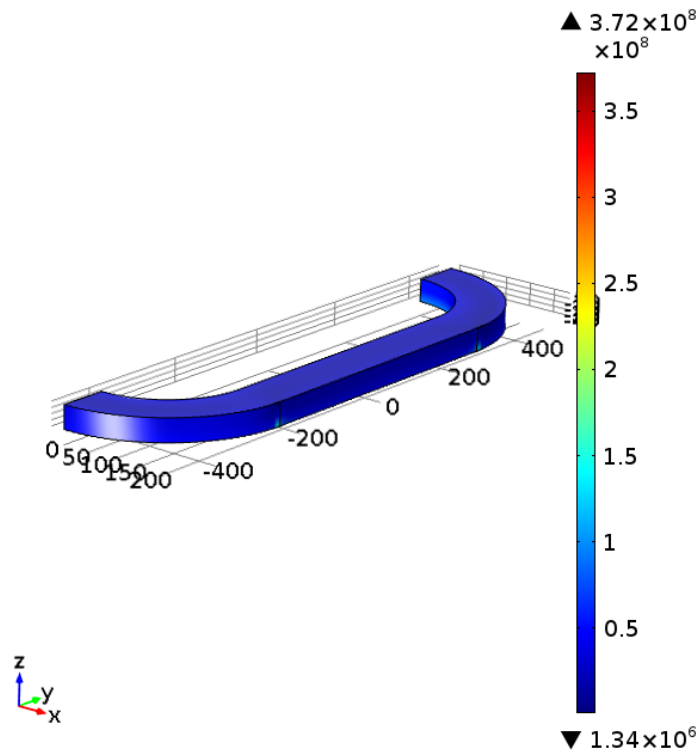


Figure 2-13 Von Mises stress in the coil due to thermal stress after cooling down the coil from room temperature to $T = 30\text{ K}$ and conducting 1 W of heat away from the coil. The unit of the stress in $[\text{Pa}]$ and it should be noted that the maximum of the color bar is equivalent to 372 MPa . This is however an artifact of a challenging meshing of the coil geometry, which is explained in a following graph. The Von Mises stress level is around $30 - 60\text{ MPa}$. Only the coil domain is shown in the figure.

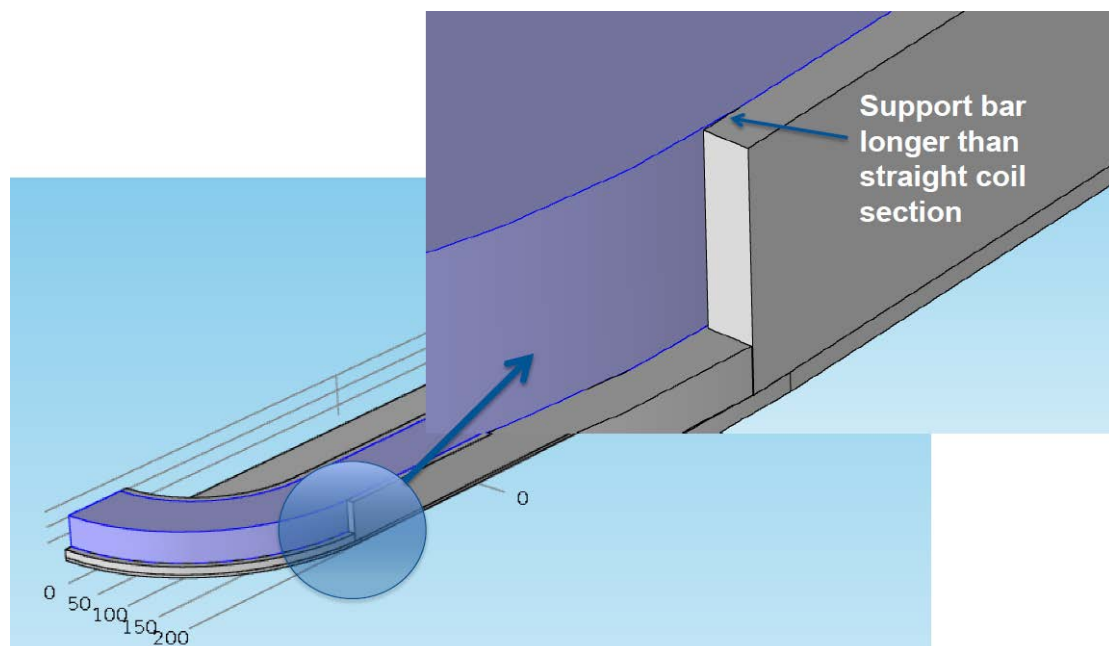


Figure 2-14 Illustration of the difficult meshing region of the geometry of the MgB_2 race track coil. The stainless steel support bar is extending further than the coil, but the intersection line will change as the coil is deformed resulting in a difficult meshing situation. Thus the result along the intersection line is neglected as being a mesh artifact.

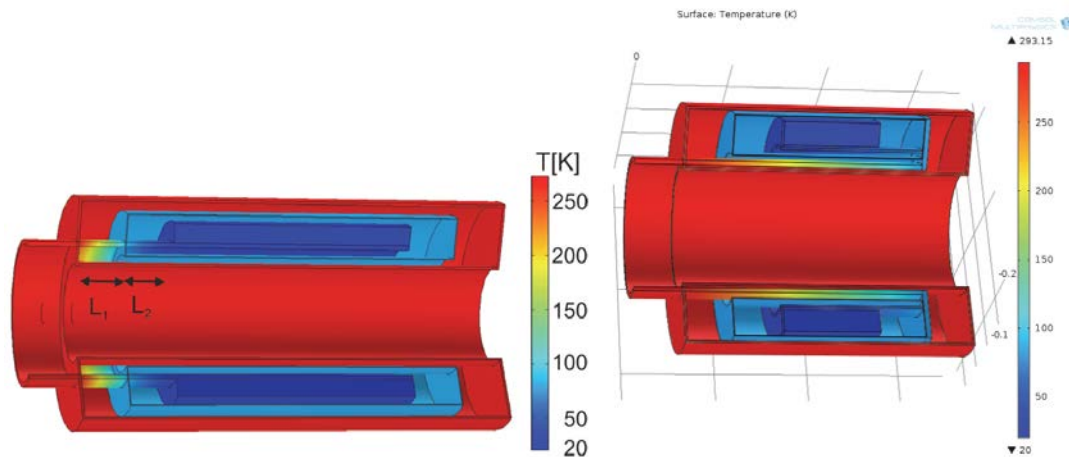


Figure 2-15 Illustration of torque tubes transmitting the generator torque from room temperature and to the support structure of the coil at low temperature of $T = 20$ K. Reproduced from deliverable D3.42 fig 4-5 and 4-6 (Liu, et al., 2013).

2.4 Discussion

The thermal stress analysis is showing that the aircored MgB_2 coil can be supported by the stainless steel bars at the side and stainless steel lid on top and bottom of the coil. This design was used in the MgB_2 coil demonstration, but it was realized in a simpler and less compact design.

The air-cored MgB_2 coil shown above was seen as the “light weight” superconducting generator option at the beginning of the INN WIND.EU project. Such coils would have to be integrated into a cryostat by a torque transfer tube as proposed in the deliverable D3.42 (Liu, et al., 2013) and shown in Figure 2-15.

It was however concluded from the generator optimization work as well as feedback from work package 1 that only very small cost saving would result from reduced generator mass, because the resonance of the rotor excitation is intersecting with resonances in the foundation for the 10 MW INN WIND.EU reference turbine and foundation. This resulted in a reformulation for the superconducting generator design philosophy to strive for “Cheap and not too heavy” (See (Abrahamsen, Liu, & Polinder, Direct drive superconducting generators for INN WIND.EU wind turbines, 2017). This philosophy changed the generator topology to include as much magnetic steel laminate in the superconducting generators as possible in order to reduce the usage of expensive superconducting wire. This is done by extending the steel laminates through the superconducting rotor field coils all the way to the physical air gap of the generator. A result of that is that the air cored coil support shown above cannot be used.

Instead one will have to construct a cryostat that surrounds the superconducting field coils and have a warm pole piece in the middle. This kind of cryostat was investigated in the SUPRApower project (Marino, Pujana, & Sarmiento, 2016) by the Karlsruhe Institute of Technology (KIT) and it was decided to make a projection of the SUPRApower cryostat and cooling system onto the INN WIND.EU generators in order not to duplicate the work of SUPRApower. The SUPRApower cryostat and cooling concept is described in section 3.

2.5 Conclusion on air cored coil support

The philosophy of “cheap and not too heavy” superconducting generators resulted in the need for iron cored design and the initial work on the mechanical support of air-cored coils was discontinued. It was decided to project the cryostat and cooling system of the SUPRApower project onto the INN WIND.EU generators in order not to duplicate their work.

3 MECHANICAL SUPPORT OF MgB_2 COILS IN 10 MW GENERATOR

The projection of the SUPRApower cryostat and cooling system onto the INN WIND.EU MgB_2 superconducting generators has been described in deliverable D3.11 (Abrahamsen, Liu, & Polinder, Direct drive superconducting generators for INN WIND.EU wind turbines, 2017), but some additional details are discussed in this section.

The SUPRApower cryostat is based on an outer stainless steel vacuum chamber, which is holding a cryocooler cold head in the wall as shown on Figure 3-1. The cold head is cooling the coil by the heat conducting through a copper plate connected to the second stage of the cold head and the first stage is connected to the active cooled shield, which is removing most of the heat radiation coming from the cryostat walls.

The coil and active shield are fixed inside the cryostat using carbon fibre rods, which are providing a good mechanical contact, but a low thermal contact. The purpose of the carbon fibre rods is only to keep the coil in the centre position of the cryostat as the magnetic steel laminates of the generator are magnetized and not to transmit the full torque of the generator to the superconducting coils, since most of the generator forces are related to the magnetic steel. The advantage of this is large seen from a generator construction point of view, because the steel laminates are transmitting the torque as in conventional machines. It also means that the torque tube illustrated on Figure 2-15 is not needed, which is simplifying the mechanical design of the cryostat, but the thermal design becomes more complicated since the warm bore result in a larger heat inflow to the superconducting coil and a need for more cooling power.

The cold head used by SUPRApower is a COOLPOWER 10 MD from Oerlikon (Oerlikon, 2017). This is connected to a COOLPAK 6000 HMD / 6200 HMD helium compressor moving helium gas forth and back to the cold head with a frequency of about 1 Hz in metal below flexible tubes. In general the helium compressors designed for cryogenic cold heads cannot be rotated, since the compressor contains oil, which will leak into the helium lines if turned upside down. Thus the helium compressor in a superconducting wind turbine have to be positioned in the static frame in order to operate. In the SUPRApower project this was solved by placing the helium compressor in the nacelle and to place a rotating gas coupling through which the helium is transferred into the rotating frame and up to the cold heads positioned on the inner ring of the 10 MW direct drive generator shown in Figure 3-2. This generator design has the superconducting coils positioned on top of the salient poles on the inner ring and an air-cored copper armature winding on the outer ring.

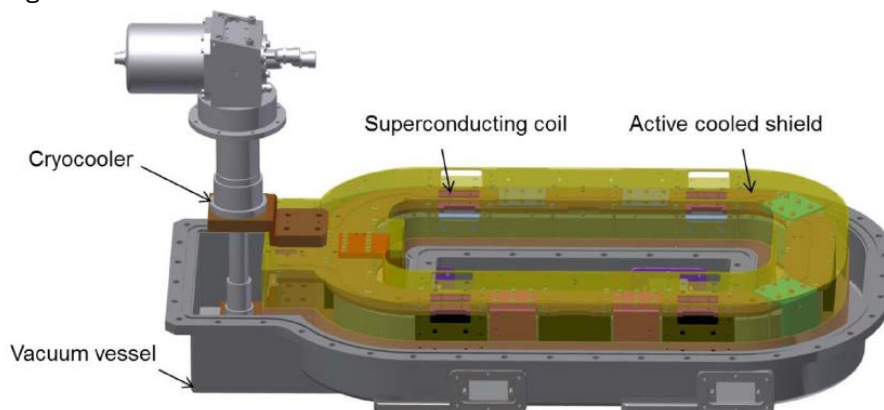


Figure 3-1 Illustration of SUPRApower cryostat holding a MgB_2 field coil and a cryocooler cold head (left) to keep the coil at $T = 20$ K. The cryostat is closed by a top lid (not shown) and the magnetic steel laminate pole piece will go through the hole in the middle of the cryostat. The transparent yellow structure is an active cooled shield, which is connected to the first stage of the cold head keeping it at about $T = 80$ K. The second stage of the cryocooler cold head is connected to copper structures providing the cooling of the MgB_2 coil.

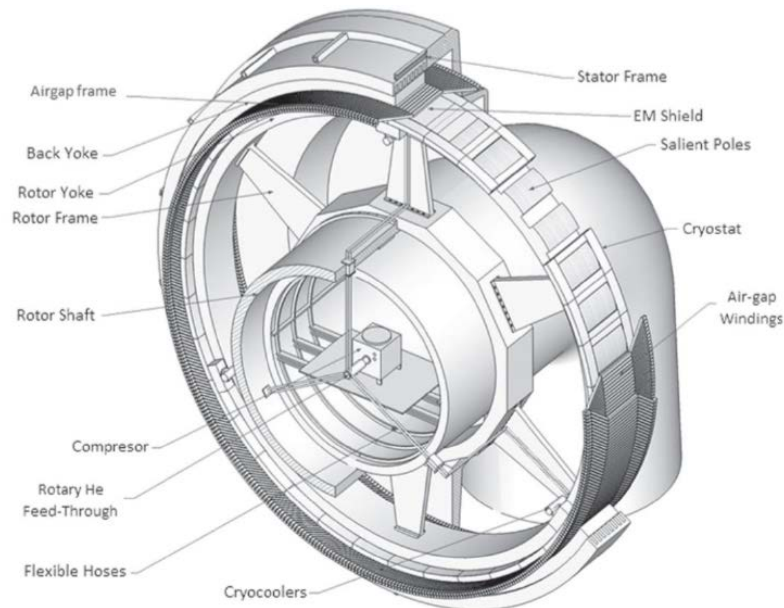


Figure 3-2 Illustration of how the helium compressor is placed in the static frame in the center of the hub and is connected to the cold heads on the inner rim of the generator. Reproduced from Fig 1 in (Marino, Pujana, & Sarmiento, 2016)

3.1 Scaling of the SUPRApower cryostat to the INN WIND.EU generator

The details of the SUPRApower cryostat has been reported by Sun (Sun, Sanz, & Neumann, 2015) and the heat load on the Oerlikon COOLPOWER 10 MD cold heads has been determined. The main contributions to the heat load are:

- 1) AC losses experienced in the MgB_2 coil
- 2) Heat dissipation and conduction through the current leads going to the coil from ambient temperature.
- 3) Heat inflow to the coil coming from heat radiation, heat conduction through the mechanical support and finally the pressure of the vacuum in the cryostat (remaining gas).

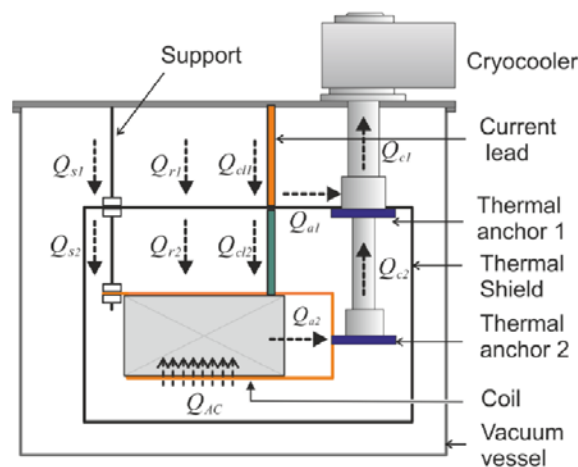


Figure 3-3 Illustration of the heat inflow of the SUPRApower cryostat. Reproduced from Fig. 5 in (Sun, Sanz, & Neumann, 2015).

The estimated losses of the SUPRApower cryostat as illustrated in Figure 3-3 and listed in Figure 3-4. The question is how to scale them to match the INN WIND.EU generators. This is done by assuming that all the losses except the current lead loss Q_{cl} will be proportional with the circumferential length of the race track coil, whereby the main scaling is done by the ratio of lengths of the straight section of the race track coils in the different generators. The losses in the current leads Q_{cl} will scale with the operation current I of the coil as given by

$$Q_{cl} = I\sqrt{L_0(T_a^2 - T_s^2)} \quad (3-1)$$

where L_0 is the Lorentz number, T_a is the ambient temperature at the cryostat wall and T_s is the shield temperature (Sun, Sanz, & Neumann, 2015). Thus the current lead loss is scaled with the ratio between the operation currents of the superconducting field windings of the different generators.

	subscript	Q_s	Q_r	Q_{AC}	Q_{cl}	Q_a	T_a
Unit		W	W	W	W	W	K
Shield	1	5.11	1.07	0	3	8.26	80
Coil	2	0.79	0.1	1.25	0.03	2.17	20

Figure 3-4 Losses of the SUPRApower cryostat operating at $T = 20$ K and indices are relating to Figure 3-3. Reproduced from table 2 in (Sun, Sanz, & Neumann, 2015).

	Q_s [W]	Q_r [W]	Q_{AC} [W]	Q_d [W]	Q_a [W]	T_a [K]	L_{stack} [m]	I_{coil} [A]	Q_{Total} [W]	Cold head	Comp power [kW]	Coldhead Compres [k€]	Weight [kg]	Volume [m ³]
SUPRAPower	Shield	5,11	1,07	0	3	80	0,52	95						
	Coil	0,79	0,1	1,25	0,03	20	0,52	95						
INN WIND 10 MW	Shield	11,1	2,3	0,0	11,8	80	1,13	374	1413	13				
	Coil	1,7	0,2	2,7	0,1	20	1,13	374	267	15	103,8	222,5	1840	1,7
INN WIND 20 MW	Shield	22,1	4,6	0,0	12,2	80	2,25	386	2803	25				
	Coil	3,4	0,4	5,4	0,1	20	2,25	386	676	38	262,7	562,9	4653	4,3

Figure 3-5 Projection of SUPRAPower cryostat and cooling technology onto the INN WIND.EU MgB₂ generators. Reproduced from table 9-2 in (Abrahamsen, Liu, & Polinder, Direct drive superconducting generators for INN WIND.EU wind turbines, 2017).

4 DISCUSSION

The result of the scaling has been reported in deliverable D3.11 and is also shown in Figure 3-5. This estimate is of course not a full design and contains some uncertainty, but it is giving a reasonable starting point for the evaluation of the cost of the cooling system by the determination of the cold head and compressor count. The authors have not been able to find a cost analysis of the SUPRApower concept and in Deliverable D3.11 an approximate quotation was obtained from Oerlikon on a 10 MD coldhead and a COOLPAK 6000 compressor. It was assumed that the INN WIND.EU cost of the cold head and the compressor would be half of that in case large numbers were ordered (This assumption is purely done by the authors and is not confirmed by Oerlikon).

Secondly the cost of the cryostat was not estimated from the materials bill, but determined as a target by using the cryostat cost estimation for a low temperature superconducting direct drive generator design done by Y. Liu *et. al.* (Liu, et al., 2015). Liu *et. al.* determined a cryogenic system cost of 600 k€, which has been used in the INN WIND.EU MgB₂ generator optimization work of D3.11 (Abrahamsen, Liu, & Polinder, Direct drive superconducting generators for INN WIND.EU wind turbines, 2017). The cost of the cryostats for the 10 MW INN WIND.EU generator was therefore estimated to be the design cost of the cryo-system subtracted the cost of the cold head and the helium compressors. The result is

$$C_{\text{cryostat}} = C_{\text{cryosystem}} - C_{\text{coldhead + compressor}} = 600 \text{ k€} - 223 \text{ k€} = 377 \text{ k€}$$

More work is needed to confirm the accuracy of this number, but it is giving an indication of the distribution between the cryostats and cooling machine cost.

What is learned from the above analysis is also that the cost of the cryostat and cooling system is considerably higher than the cost of the MgB₂ superconductor, which for the 10 MW MgB₂ INN WIND.EU generator is estimated to be about 85 k€ corresponding to about 22 km of MgB₂ wire. Thus further work in reducing the Levelized Cost of Energy (LCoE) of the MgB₂ direct drive wind turbine generator has to be focused on the reduction of the cryo-system cost.

This calls for generator optimization methods taking both the electromagnetic as well as the cryogenic physics into account at the same time. The current optimization method of the INN WIND.EU project was only optimizing the electromagnetics assuming the cryogenic system as fixed and constant. Secondly optimization methods with possible restrictions on the total mass of the generator would also be beneficial, but a challenge will be to couple the generator active materials performance to the design of the generator structural support.

5 CONCLUSION

A simple model for estimating the dimensions of the mechanical support of a superconducting race track coil has been provided and used to determine the layout of the INNWIND.EU MgB₂ race track coil demonstrator from a mechanical and thermal point of view.

The change of the INNWIND.EU generator design philosophy from “light weigh” and to “cheap and not to heavy” has caused the original air cored coil support to be discontinued and the design of having a warm steel laminate bore was pursued instead. Such a design is similar to the cryostat design of the SUPRApower project (Marino, Pujana, & Sarmiento, 2016) and it was decided to make a projection of their design onto the INNWIND.EU MgB₂ generators instead of replicating their work. This report is describing how the project of the cryogenic system was done and also how an approximate cost was estimated.

More work on combined optimization of the electromagnetics of the generator and the cryogenics system is recommended as further steps in order to reduce the Levelized Cost of Energy of the MgB₂ superconducting generators, since the cost of the cryosystem is now higher than the cost of the MgB₂ superconducting windings used in the coils.

REFERENCES

- Abrahamsen, A. (2016). Wind generator projects based on MgB2 superconductors. In R. Flükiger, *MgB2 superconducting wires: Basics and applications* (pp. 611-640). World Scientific.
- Abrahamsen, A., Liu, D., & Polinder, H. (2017). *Direct drive superconducting generators for INN WIND.EU wind turbines*. INN WIND.EU Deliverable report D3.11.
- Abrahamsen, A., Magnusson, N., Jensen, B., Liu, D., & Polinder, H. (2014). Design of an MgB2 race track coil for a wind generator pole demonstration. *Journal of Physics: Conference Series* 507, 032001.
- Abrahamsen, A., Magnusson, N., Liu, D., Stehouwer, E., Hendriks, B., & Polinder, H. (2014). Design study of a 10 MW MgB2 superconductor direct drive wind turbine generator. *Proceedings of EWEA 2014. European Wind Energy Association (EWEA)*. EWEA.
- AML. (2017, October). <http://amlsuperconductivity.com/applications/energy/doe-approved-wind-turbine-solution/>.
- Columbus Superconductors. (2017, November). <http://www.columbussuperconductors.com/>.
- Kalsi, S. (2014). Superconducting wind turbine generator employing MgB2 windings both on rotor and stator. *IEEE Transaction on applied superconductivity* 24, 5201907.
- Keysan, O., & Mueller, M. (2015). A modular and cost effective superconducting generator design for offshore wind turbines. *Superconductor Science and Technology* 28, 034004.
- Liu, D., Abrahamsen, A., McDonald, A., Penzkofer, A., Meyers, A., Dolacinski, A., . . . Polinder, H. (2013). *First assessment of performance indicators of superconducting- and pseudo magnetic direct drive generators*. INN WIND.EU Deliverable report D3.42.
- Liu, D., Polinder, H., Abrahamsen, A., & Ferreira, J. (2017). Topology Comparison of Superconducting Generators for 10-MW Direct-Drive Wind Turbines: Cost of Energy Based. *IEEE TRANSACTIONS ON APPLIED SUPERCONDUCTIVITY, VOL. 27*, 5202007.
- Liu, Y., Qu, R., Wang, J., Fang, H., Zhang, X., & Chen, H. (2015). Influences of generator parameters on fault current and torque in a large-scale supersuperconducting wind generator. *IEEE Transactions on Applied Superconductivity*, 5204309.
- Magnusson, N., Hellesø, S., Paulsen, M., Eliassen, J., & Abrahamsen, A. (2016). *Fabrication of MgB2 Coils – A superconducting generator pole demonstrator*. INN WIND.EU deliverable report D3.13.
- Marino, I., Pujana, A., & Sarmiento, G. (2016). Lightweight MgB2 superconducting 10 MW wind generator. *Supercond. Sci. Technol.* 29, 024005.
- Oerlikon. (2017, November). www.oerlikon.com.
- Sun, J., Sanz, S., & Neumann, H. (2015). Conceptual design and thermal analysis of a modular cryostat for one single coil of a 10 MW offshore superconducting wind turbine. *IOP Conf. Series: Materials Science and Engineering*, 101, (p. 012088).